Continuum effects and three-nucleon forces in neutron-rich oxygen isotopes

G. Hagen,[1, 2] M. Hjorth-Jensen,[3, 4, 5] G. R. Jansen,[3] R. Machleidt,[6] and T. Papenbrock[2, 1]

[1]*Physics Division, Oak Ridge National Laboratory, Oak Ridge, TN 37831, USA*
[2]*Department of Physics and Astronomy, University of Tennessee, Knoxville, TN 37996, USA*
[3]*Department of Physics and Center of Mathematics for Applications, University of Oslo, N-0316 Oslo, Norway*
[4]*National Superconducting Cyclotron Laboratory, Michigan State University, East Lansing, MI 48824-1321, USA*
[5]*Department of Physics and Astronomy, Michigan State University, East Lansing, MI 48824, USA*
[6]*Department of Physics, University of Idaho, Moscow, ID 83844, USA*

We employ interactions from chiral effective field theory and compute binding energies, excited states, and radii for isotopes of oxygen with the coupled-cluster method. Our calculation includes the effects of three-nucleon forces and of the particle continuum, both of which are important for the description of neutron-rich isotopes in the vicinity of the nucleus ^{24}O. Our main results are the placement of the neutron drip-line at ^{24}O, the assignment of spins, parities and resonance widths for several low-lying states of the drip-line nucleus, and an efficient approximation that incorporates the effects of three-body interactions.

Introduction. – Neutron-rich oxygen isotopes are particularly interesting nuclei. First, the nuclei ^{22}O and ^{24}O exhibit double magicity at the neutron numbers $N = 14$ and $N = 16$, respectively, see for example Refs. [1–3]. Second, oxygen is the heaviest element for which the neutron drip line is established experimentally. The recent experiments [4, 5] show clearly that the nuclei ^{25,26}O are unbound, thus making ^{24}O the most neutron-rich bound isotope of oxygen. The spectroscopy of the drip line nucleus ^{24}O was studied in a recent experiment [6]. One of the exciting results of this study is a state with an unknown spin and parity at about 7.5 MeV of excitation energy. Theoretical studies in this region of the nuclear chart are challenging [7–10]. Volya and Zelevinsky [7] employed an empirical two-body shell-model interaction (above the core of ^{16}O) and included the particle continuum in their calculation of neutron-rich oxygen isotopes. Otsuka *et al.* [9] included three-nucleon forces (3NFs) within the *sd*-shell model (keeping ^{16}O as a core with empirical single-particle energies) and found that three-body forces yield ^{24}O at the neutron drip line. The *ab initio* computations of neutron-rich oxygen isotopes by Hagen *et al.* [8] employed microscopic interactions from chiral effective field theory [11], had no core, but were limited to nucleon-nucleon (NN) interactions. Thus, we are still lacking a complete computation of neutron rich oxygens that properly accounts for (i) the effects of three-nucleon forces, (ii) the presence of open decay channels and particle continuum, and (iii) many-nucleon correlations. It is the purpose of this Letter to fill this gap. In particular we predict the spins and lifetimes of several resonances in ^{24}O at excitation energies around 7 MeV and thereby shed light on the recent experiment [6].

Effective field theory (EFT) is the framework that allows for a consistent formulation of low-energy nuclear Hamiltonians and currents [11–13]. Within chiral EFT, 3NFs are important contributions that enter at next-to-next-to-leading order in the power counting. In light nuclei, our understanding of 3NFs has improved considerably over the past decade, and nuclear binding energies, spectra and decays cannot be understood without them [14–18]. The study of the role of 3NFs in medium-mass nuclei and exotic, neutron-rich nuclei is a frontier in contemporary nuclear structure theory. To date, the full inclusion of 3NFs is limited to *p*-shell nuclei. For heavier nuclei or nuclear matter, several approaches [9, 10, 19–21] employ a normal-ordered approximation [22], resulting in a medium-dependent two-body potential that includes effects of the 3NFs. Furthermore, the employed interactions are renormalization group transformations [23] of interactions from chiral EFT.

Hamiltonian and model space. – The intrinsic A-nucleon Hamiltonian used in this work reads

$$\hat{H} = \sum_{1 \leq i < j \leq A} \left(\frac{(\vec{p}_i - \vec{p}_j)^2}{2mA} + \hat{V}_{NN}^{(i,j)} + \hat{V}_{3\text{Neff}}^{(i,j)} \right) . \quad (1)$$

Here, the intrinsic kinetic energy depends on the mass number A. The potential $\hat{V}_{NN}$ is the chiral NN interaction developed by Entem and Machleidt [11] at next-to-next-to-next-to-leading order (N^{3}LO) within chiral EFT. The potential $\hat{V}_{3\text{Neff}}$ is the in-medium NN interaction derived by Holt *et al.* [19] from the leading order chiral 3NF by integrating one nucleon over the Fermi sea (i.e. up to the Fermi momentum k_F) in symmetric nuclear matter. The leading chiral 3NF depends on five low-energy constants (LECs). The LECs $c_1 = -0.81$ GeV^{-1}, $c_3 = -3.20$ GeV^{-1}, and $c_4 = 5.40$ GeV^{-1} appear also in the two-pion exchange part of the chiral NN interaction and have the same values as in the N^{3}LO NN potential we employ [11]. The remaining LECs of the 3NF are set at $c_D = -0.2$ and $c_E = 0.71$ together with $\Lambda_\chi = 0.7$ GeV. For the oxygen isotopes considered in this work we apply the Fermi momentum $k_F = 1.05$ fm^{-1} in our potential $\hat{V}_{3\text{Neff}}$. Consistent with the NN force, the effective cutoff

for the 3NF is $\Lambda = 500$ MeV.

Let us comment on our phenomenological two-body potential $\hat{V}_{3\text{Neff}}$ that contains effects of 3NFs. The normal-ordered approximation of 3NFs [9, 21, 22] still requires one to compute an enormous number of three-body matrix elements. This poses a great challenge for the large model spaces we need to consider. The approach of this Letter is thus simpler: The summation over the third particle is performed in momentum space *before* the transformation to the oscillator basis takes place [39]. This procedure avoids the costly computation of three-body matrix elements in large oscillator spaces, but it introduces an uncontrolled approximation by replacing the mean-field of a finite nucleus by that of symmetric nuclear matter. To correct for this approximation, we adjusted the LEC c_E away from the optimal value established in light nuclei [25].

The coupled-cluster method is essentially a similarity transformation of the Hamiltonian with respect to a reference state. This method is accurate and efficient for nuclei with closed (sub-)shells [26–28]. We compute the ground states of ^{16,22,24,28}O within the singles and doubles approximation, while three-particle–three-hole ($3p$-$3h$) excitations are included in the Λ-CCSD(T) approach of Ref. [30]. For excited states in these closed-shell isotopes we employ the equation-of-motion (EOM) coupled-cluster method with singles and doubles. The open-shell nuclei ^{15,17,21,23,25}O are computed within the particle attached/removed EOM formalism, and we employ the two-particle attached EOM formalism [31] for the nuclei ^{18,26}O. For details about our implementation see Ref. [29]. These EOM methods work very well for states with dominant $1p$-$1h$, $1p$, $1h$, and $2p$ structure, respectively. We use a Hartree-Fock basis built in 17 major oscillator shells and varied the oscillator spacing $\hbar\omega$ between 24 MeV and 32 MeV. Well converged energy minima are found at $\hbar\omega \approx 28$ MeV for all oxygen isotopes. Open decay channels and the particle continuum near the dripline nucleus ^{24}O are included within the Gamow shell model [32, 33]. The single-particle bound and scattering states result from diagonalizing a spherical Woods-Saxon Hamiltonian in a discrete momentum basis in the complex plane [33, 34]. In the case of computing resonances in ^{24}O we used 35 mesh points for the $d_{3/2}$ partial wave on a rotated/translated contour in the complex momentum plane as described in Ref.[35]. The excited states we compute in ^{22,24}O are dominated by $1p$-$1h$ excitations and continuum mixing from other partial waves is small. They result as solutions of a complex-symmetric eigenvalue problem, and the imaginary part of the energy yields the width of the state. In computing radii we discretized the real momentum axis with 40 points for the neutron and proton partial waves closest to the threshold. This guarantees the correct exponential decay of matter and charge densities at large distances.

Results. – Figure 1 shows the ground-state energies of the computed oxygen isotopes (red squares) compared with experimental data (black circles) and results limited to chiral NN interactions only (blue diamonds). For the isotopes around ^{16}O, NN interactions alone already describe separation energies rather well, and the inclusion of effects of 3NFs mainly changes underbinding into overbinding. For the more neutron-rich oxygen isotopes, the 3NFs significantly change the systematics of the binding energies, and energy differences are particularly well reproduced. The nuclei ^{25,26}O are unbound with respect to ^{24}O by about 0.4 MeV and about 0.1 MeV, respectively, in good agreement with experiments [4, 5]. We predict ^{28}O to be unbound with respect to ^{24}O by about 4 MeV and with a resonant width of about 1 MeV. The extremely short life time of ^{28}O poses a challenge for experimental observation. The energy difference between light and heavy oxygen isotopes is not correctly reproduced when compared to data. We believe that this is due to the fact that our interaction $\hat{V}_{3\text{Neff}}$ is based on symmetric nuclear matter. For smaller values of k_F, the ground-state energy of the lighter oxygen isotopes is increased (and can be brought to good agreement with data), while the heavier isotopes are significantly underbound. The value we chose for k_F is thus a compromise.
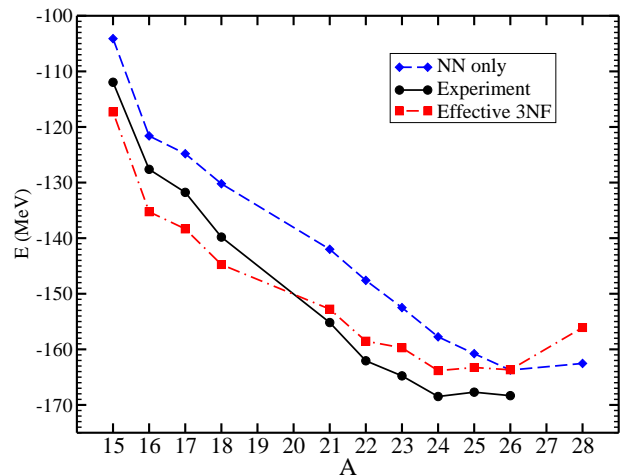

FIG. 1: (Color online) Ground-state energy of the oxygen isotope ^{A}O as a function of the mass number A. Black circles: experimental data; blue diamonds: results from nucleon-nucleon interactions; red squares: results including the effects of three-nucleon forces.

Let us comment on our computation of oxygen isotopes with open shells. First, we solve the CCSD equations for the Hamiltonian (1) of the closed-shell reference state, but employ the mass number $A \pm 1$ in the intrinsic kinetic energy. In a second step, we add (remove) a neutron within the particle attached (removed) EOM. This procedure ensures that the final result is obtained for the intrinsic (i.e., translationally invariant) Hamiltonian of $^{A\pm1}$O. The $J^\pi = 1/2^+$ ground state energy

of ^{23}O, shown in Fig. 1, resulted from using particle-removal EOM from ^{24}O. For ^{18,26}O, we performed a two-neutron attached EOM computation based on the reference states for ^{16,24}O, the latter being computed with the mass number $A = 18, 26$ in the intrinsic kinetic energy. This approach is unproblematic for separation energies but it introduces an error in the computation of resonance widths. Our computation of ^{25}O within the neutron attached EOM employs a Gamow basis. Here the continuum threshold is incorrectly set by the closed-shell reference of ^{24}O, computed with the mass number $A = 25$ in the intrinsic kinetic energy. Clearly, this introduces a small error by shifting the scattering threshold, and thereby affects the widths of resonance states that are very close to the threshold. In Ref. [36] we showed that the coupled-cluster wave function factorizes into an intrinsic and a center-of-mass part. The center-of-mass wave function is to a very good approximation a Gaussian with a frequency $\hbar\tilde{\omega} \approx 14$ MeV for ^{24}O. Thus, we estimate the error introduced in the scattering threshold of ^{25}O to be $\frac{3}{4}\hbar\tilde{\omega}/A \approx 0.4$ MeV.

Figure 2 shows the excitation spectra of neutron-rich oxygen isotopes and compares the results limited to chiral NN interactions (blue lines) to the results obtained with our inclusion of 3NFs (red lines), and to experimental data (black lines) [40]. The particle continua above the scattering thresholds are shown as gray bands. Calculations limited to NN interactions yield the correct level ordering but very compressed spectra when compared to data, and all the computed excited states are well bound with respect to the neutron emission thresholds. However, the inclusion of 3NFs increases the level spacing and significantly improves the agreement with experiment. Several of the excited states are resonances in the continuum, and the proximity of the continuum is particularly relevant for the dripline nucleus ^{24}O. Here, the Gamow basis is essential for a proper description of the excited resonant states. In ^{24}O we find three resonant states near the unknown experimental state at about 7.5 MeV of excitation energy [6]. The excited $J^\pi = 3/2^+$ state in ^{23}O is computed as a neutron attached to ^{22}O, while the excited $J^\pi = 5/2^+$ state is computed by neutron removal from ^{24}O. Since we are interested in the excitation energy relative to the ground state we compute the $J^\pi = 1/2^+$ ground state either by adding or removing a particle, consistent with the particular excited state. For the lighter isotopes ^{15,16,17}O, our inclusion of 3NFs yields only smaller changes to the spectra when compared with results from NN interactions only.

For the closed-shell nucleus ^{24}O we also computed resonance widths of excited states that are dominated by $1p$-$1h$ excitations from the $s_{1/2}, d_{5/2}$ hole to the $d_{3/2}$ particle orbitals. Table I shows that the first $J^\pi = 2^+$ and 1^+ excited states agree well with experimental data, both for the excitation energy and the resonance widths. The rather small widths and quasi-bound nature of these
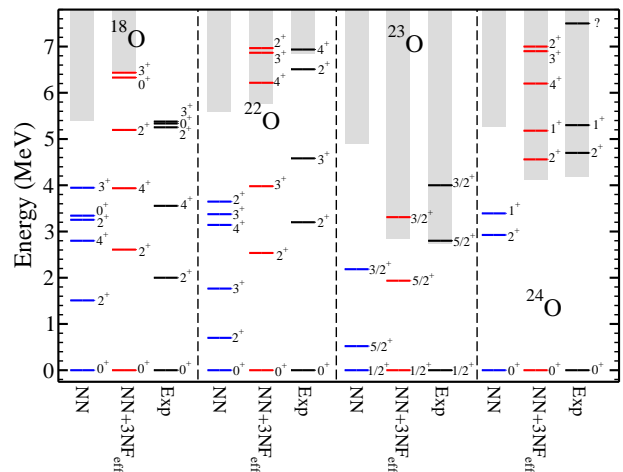

FIG. 2: (Color online) Excitation spectra of oxygen isotopes computed from chiral nucleon-nucleon interactions, with inclusion of the effects of three-nucleon forces, and compared to data.

J^π	2_1^+	1_1^+	4_1^+	3_1^+	2_2^+	1_2^+
E_{CC}	4.56	5.2	6.2	6.9	7.0	8.4
E_{Exp}	4.7(1)	5.33(10)				
Γ_{CC}	0.03	0.04	0.005	0.01	0.04	0.56
Γ_{Exp}	$0.05^{+0.21}_{-0.05}$	$0.03^{+0.12}_{-0.03}$				

TABLE I: Excited states in ^{24}O computed within EOM-CCSD compared to experimental data from Ref. [6]. Energies and widths are in MeV.

states can be attributed to the large angular momentum barrier of the $d_{3/2}$ orbital, together with neutron pairing effects. Above these 2_1^+ and 1_1^+ resonances we find several states with spin and parity $J^\pi = 1^+$ to 4^+ and excitation energies ranging from 6.2 MeV to 8.4 MeV. The small ratio $E_{4_1^+}/E_{2_1^+} \approx 1.36$ and the relatively high energy $E_{2_1^+}$ lend theoretical support to the doubly magic nature of ^{24}O [3]. The low experimental resolution of the resonance at 7.5 MeV let Hoffman et $al.$ [6] to speculate that this resonance could be a superposition of narrow resonances with spins and parity $J^\pi = 1^+$ to 4^+. Our calculation clearly supports this suggestion, except for the 1_2^+ state which we find at 8.4 MeV of excitation energy and with a width of 0.56 MeV.

Figure 3 shows the computed point matter and point charge radii for the neutron-rich isotopes $^{21-24}$O with a comparison to the experimental data (Ref. [37] for ^{21}O and Ref. [38] for ^{22,24}O). This computation employs the intrinsic density with respect to the center of mass. Our computed radii agree very well with experiment for the odd isotopes ^{21,23}O, while for ^{22}O we underestimate the radii compared to experiment. We also computed the point matter radii from NN interactions only (blue di-

amonds). In this case the radii overestimate the data for ^{21,23}O, while ^{22,24}O they are closer to the results with effects of 3NF's included. The computed charge radii clearly exhibit an odd-even staggering consistent with the shell closures at neutron numbers $N = 14, 16$. For ^{16}O, the computed point matter and charge radii are 2.23 fm and 2.24 fm, respectively. This is about 0.3 fm smaller than experiment and consistent with the computed overbinding and the increased neutron and proton separation energies.
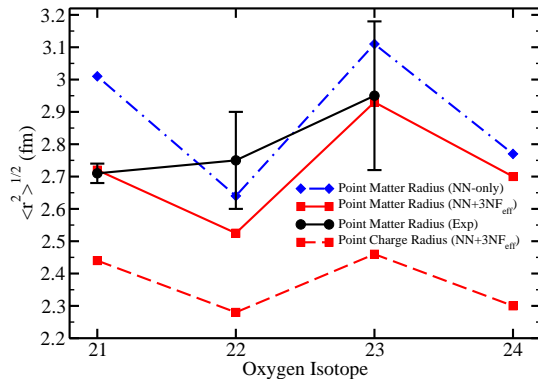

FIG. 3: (Color online)Point matter and point charge radii of neutron rich oxygen isotopes computed from chiral nucleon-nucleon interactions, with inclusion of the effects of three-nucleon forces, and compared to data.

Summary. – We employed interactions from chiral effective field theory, performed coupled-cluster computations of oxygen isotopes, and included effects of the particle continuum and of three-nucleon forces. Three-nucleon forces were approximated as in-medium nucleon-nucleon forces. This approach is computationally feasible and in keeping with the spirit of effective field theory. Compared to computations based on nucleon-nucleon interactions alone, the included 3NFs yield a significant improvement in binding energies and spectra. Our results confirm that chiral interactions yield the neutron drip line at ^{24}O, and we are able to compute spin, parities and resonance widths for several excited states close to the dripline. In particular, we compute several long-lived resonances at about 7 MeV of excitation energy in ^{24}O.

[1] P. Thirolf *et al.*, Phys. Lett. B **485**, 16 (2000).
[2] C. R. Hoffman *et al.*, Phys. Lett. B **672**, 17 (2009).
[3] R. Kanungo *et al.*, Phys. Rev. Lett. **102**, 152501 (2009).
[4] C. R. Hoffman *et al.*, Phys. Rev. Lett. **100**,152502 (2008).
[5] E. Lunderberg *et al.*, Phys. Rev. Lett. **108**, 142503 (2012).
[6] C. R. Hoffman *et al.*, Phys. Rev. C **83**, 031303(R) (2011).
[7] A. Volya and V. Zelevinsky, Phys. Rev. Lett. **94**, 052501 (2005).
[8] G. Hagen *et al.*, Phys. Rev. C **80**, 021306 (2009).
[9] T. Otsuka *et al.*, Phys. Rev. Lett. **105**, 032501 (2010).
[10] J. D. Holt and A. Schwenk, arxiv:1108:2680.
[11] D. R. Entem and R. Machleidt, Phys. Rev. C **68**, 041001(R) (2003).
[12] E. Epelbaum, H. W. Hammer, and Ulf-G. Meissner, Rev. Mod. Phys. **81**, 1773 (2009).
[13] R. Machleidt and D. R. Entem, Phys. Rep. **503**, 1 (2011).
[14] R. B. Wiringa and S. C. Pieper, Phys. Rev. Lett. **89**, 182501 (2002).
[15] P. Navrátil and W. E. Ormand, Phys. Rev. Lett. **88**, 152502 (2002).
[16] P. Navrátil *et al.*, J. Phys. G **36**, 083101 (2009).
[17] E. Epelbaum *et al.*, Phys. Rev. Lett. **106**, 192501 (2011).
[18] P. Maris *et al.*, Phys. Rev. Lett. **106**, 202502 (2011).
[19] J. W. Holt, N. Kaiser, and W. Weise, Phys. Rev. C **79**, 054331 (2009); *ibid.* Phys. Rev. C **81**, 024002 (2010).
[20] K. Hebeler and A. Schwenk, Phys. Rev. C **82**, 014314 (2010); K. Hebeler *et al.*, Phys. Rev. C **83**, 031301 (2011).
[21] R. Roth *et al.*, Phys. Rev. Lett. **107**, 072501 (2011).
[22] G. Hagen *et al.*, Phys. Rev. C **76**, 034302 (2007).
[23] S. K. Bogner, T. T. S. Kuo, and A. Schwenk, Phys. Rep. **386**, 1 (2003); S. K. Bogner, R. J. Furnstahl and R. J. Perry, Phys. Rev. C **75**, 061001 (2007).
[24] J. Menéndez, D. Gazit, and A. Schwenk, Phys. Rev. Lett. **107**, 062501 (2011).
[25] D. Gazit, S. Quaglioni, and P. Navrátil, Phys. Rev. Lett. **103**, 102502 (2009).
[26] F. Coester, Nucl. Phys. **7**, 421 (1958); F. Coester and H. Kümmel, Nucl. Phys. **17**, 477 (1960); J. Čížek, J. Chem. Phys. **45**, 4256 (1966); J. Čížek, Adv. Chem. Phys. **14**, 35 (1969); H. Kümmel, K.H. Lührmann, and J.G. Zabolitzky, Phys. Rep. **36**, 1 (1978).
[27] D. J. Dean and M. Hjorth-Jensen, Phys. Rev. C **69**, 054320 (2004).
[28] R. J. Bartlett and M. Musiał, Rev. Mod. Phys. **79**, 291 (2007).
[29] G. Hagen *et al.*, Phys. Rev. C **82**, 034330 (2010).
[30] A. D. Taube and R. J. Bartlett, J. Chem. Phys. **128**, 044110 (2008); *ibid.* **128**, 044111 (2008).
[31] G. R. Jansen *et al.*, Phys. Rev. C **83**, 054306 (2011).
[32] R. Id Betan *et al.*, Phys. Rev. Lett. **89**, 042501 (2002).
[33] N. Michel *et al.*, Phys. Rev. Lett. **89**, 042502 (2002); N. Michel *et al.*, J. Phys. G **36**, 013101 (2009).
[34] Ø. Jensen *et al.*, Phys. Rev. Lett. **107**, 032501 (2011).
[35] G. Hagen *et al.*, Phys. Lett. B **656**, 169 (2007).
[36] G. Hagen, T. Papenbrock, D. J. Dean, Phys. Rev. Lett. **103**, 062503 (2009).
[37] A. Ozawa *et al.*, Nucl. Phys. A **691**, 599 (2001).
[38] R. Kanungo *et al.*, Phys. Rev. C **84**, 061304 (2011).
[39] For the approximation of two-body currents as medium-dependent one-body currents, this approach has been

used in Ref. [24].

[40] The displayed experimental levels are dominated by $1p(h)$, $2p$ or $1p$-$1h$ excitations.